ALCHEMY Jurnal Penelitian Kimia

Official Website: https://jurnal.uns.ac.id/alchemy

ISSN 1412-4092
EISSN 2443-4183

Analysis of the Impact of Sintering Temperature on the Properties of Lithium Manganese Nickel Oxide ($LiMn_{1.5}Ni_{0.5}O_4$) as a Cathode Material for Lithium-Ion Batteries

Slamet Priyono[a*], Vera Khoirunisa[b], Nanda Julistio Rahmadi[b], Ahmad Fauzi[a], and Endah Yuniarti[c]

[a]*Research Center for Advanced Material, National Research and Innovation Agency (BRIN)*
Jalan Raya Puspitek No.60, Muncul, Setu, South Tangerang 15310, Indonesia
[b]*Department of Engineering Physics, Faculty of Industrial Technology, Sumatera Institute of Technology*
Jalan Terusan Syacudu, Way Hui, Jati Agung, South Lampung 35365, Indonesia
[c]*Department of Aeronautical Engineering, University Aerospace Marshal Suryadarma*
Jalan Raya Halim Perdanakusuma, No.1, Makasar, Jakarta 13610, Indonesia

[*]*Corresponding author: slam021@brin.go.id*

DOI: 10.20961/alchemy.22.2.98301.463-471

Received 15 January 2025, Revised 26 February 2026, Accepted 14 April 2026, Published 30 September 2026

Keywords:

cathode;
$LiMn_{1.5}Ni_{0.5}O_4$;
solid-state sintering.

ABSTRACT. $LiMn_{1.5}Ni_{0.5}O_4$ cathode material was synthesized by the solid-state method at sintering temperatures of 500, 600, 700, and 800 °C. Synthesis was done by grinding and heating the material at these temperatures for 4 hours. The samples were characterized by X-ray diffraction (XRD), Field-Emission Scanning Electron Microscopy (FE-SEM), Electrochemical Impedance Spectroscopy (EIS), Cyclic Voltammetry (CV), and Charge-Discharge (CD) tests. There are three different phases, such as Lithium Manganese Oxide (LMO), Manganese Oxide (MnO_2), and Nickel Oxide (NiO) in the material from XRD analysis. FE-SEM data indicated that the disappearance of the granules and formation of denser, finer, and more uniform particles had taken place at 800 °C. Electrochemical characterization showed that the material had a low ionic resistance of 142.5 Ω and a specific capacity of 146 $mAhg^{-1}$ at 800 °C. In this study, we have successfully synthesized $LiMn_{1.5}Ni_{0.5}O_4$ by solid-state method and showed that the sintering at 800 °C may improve the electrochemical performance.

INTRODUCTION

Major advances in lithium-ion battery technology have enabled the portable electronics revolution of the last 20 years and the emergence of low-cost, handy battery electric vehicles (BEVs) (Wu *et al.*, 2019). Lithium-ion batteries are predicted to be one of the important factors in the manufacturing of electric vehicles (EVs) and plug-in hybrid electric vehicles (PHEVs) in the next years (Lv *et al.*, 2020).

One of the major challenges in lithium-ion battery manufacturing today is to find new materials that can reduce costs, extend service life, and improve safety performance (Gabrielli *et al.*, 2017). This requires the development of suitable active cathode materials, which are essential to battery performance. Recently, other materials with similar structure such as $LiNiO_2$, $LiMnO_2$ have been investigated as a possible low cost alternative to $LiCoO_2$ as cathode of lithium-ion batteries. However, $LiNiO_2$ suffers from difficulties in oxidising nickel, which affects the reversible capacity and causes degradation at high temperatures, resulting in poor cycling performance (Xie and Lu, 2020). Alternatively, Lithium Nickel Manganese Oxide ($LiNi_{0.5}Mn_{1.5}O_4$) (LMNO), a cobalt-free lithium manganese spinel modified by other transition metals, is an attractive candidate. The prism shaped 3D structure is a potential cathode material because of its high working voltage of 4.7 V and theoretical capacity of 146.7 $mAhg^{-1}$ (Bhatia *et al.*, 2020).

Thus, this work is based on the hypothesis that sintering temperature is a key factor in controlling the structural ordering and electrochemical performance of LMNO synthesised by the solid-state reaction method. In particular, an optimal sintering temperature is hypothesised to facilitate the formation of a well-crystallized spinel structure with minimal impurity phases and controlled particle growth, which in turn enhances the redox

Cite this as: Priyono, S., Khoirunisa, V., Rahmadi, N. J., Fauzi, A., and Yuniarti, E. (2026). Analysis of the Impact of Sintering Temperature on the Properties of Lithium Manganese Nickel Oxide ($LiMn_{1.5}Ni_{0.5}O_4$) as a Cathode Material for Lithium-Ion Batteries. *ALCHEMY Jurnal Penelitian Kimia*, 22(2), 463-471. doi: https://dx.doi.org/10.20961/alchemy.22.2.98301.463-471.

Copyright © 2026, Universitas Sebelas Maret, ISSN 1412-4092, e ISSN 2443-4183

reversibility, cycling stability, and high-voltage (>5 V) performance. In contrast, too high temperature may cause oxygen deficiency, cation disorder, or secondary phase formation, resulting in capacity fading and poor electrochemical stability.

LMNO will be synthesised from LiOH, MnO_2 and NiO precursors at different sintering temperatures. The effects of temperature on crystal structure, phase composition and morphology will be analysed and their correlation with electrochemical behaviour including redox processes and galvanostatic performance at high voltage will be systematically evaluated.

.

RESEARCH METHODS

The $LiNi_{0.5}Mn_{1.5}O_4$ sample was prepared by solid-state reaction using Lithium Hydroxide (LiOH), Manganese (IV) oxide, and Nickel (II) oxide. Then the raw materials were blended and ground in a mortar to smooth the rough surface of the precursor. The mixture was then sieved through a 200 mesh sieve to separate the fine and coarse particles of the Lithium Manganese Nickel Oxide (LMNO) precursor. The fine precursor was ball-milled at 25 Hz for 2 hours to get homogeneous mixing. The milled material was then sintered for 4 hours at different temperatures (500 °C, 600 °C, 700 °C, and 800 °C). Finally, the synthesised samples were characterised by X-ray diffraction (XRD) and Field-emission scanning electron microscopy (FE-SEM).

The LMNO powders obtained from the synthesis were employed to fabricate electrodes. The composition of the electrode was 80 wt% active material (LMNO), 10 wt% carbon black, and 10 wt% PVDF. These materials were mixed with DMAC (N,N-Dimethylacetamide) solvent using a magnetic stirrer and hot plate at 50 °C to prepare the slurry. The slurry was then coated on aluminium foil with a thickness of 200 µm. The coated electrodes were cut into 16 mm diameter circles and then assembled together with a separator, electrolyte and metallic Li in an Ar-filled glove box. LiPF6 was used as the electrolyte and metallic Li was used as the counter electrode. Electrochemical impedance spectroscopy (EIS) was carried out in the frequency range of 0.1-50 kHz. Cyclic voltammetry (CV) was carried out at a scan rate of 100 mV/s from 3.5 to 5.5 V and the charge-discharge (CD) test was performed from 3.0 to 5.5 V at 0.1 C

RESULTS AND DISCUSSION

The phase analysis by XRD characterisation using HighScore software shows the presence of three crystal phases in the sample, such as LMNO, Pyrolusite (MnO_2) and NiO. Among these, the main phase in the sample is LMNO. LMNO is one of the important oxide compounds for lithium-ion battery electrodes. Its outstanding lithium-ion conductivity, high stability, and stable cubic crystal structure can eventually enhance battery performance. On the other side, the Nickel Oxide and Pyrolusite (MnO_2) phases are residual precursors that did not convert to LMNO during sintering. The XRD characterisation results are presented in Figure 1.

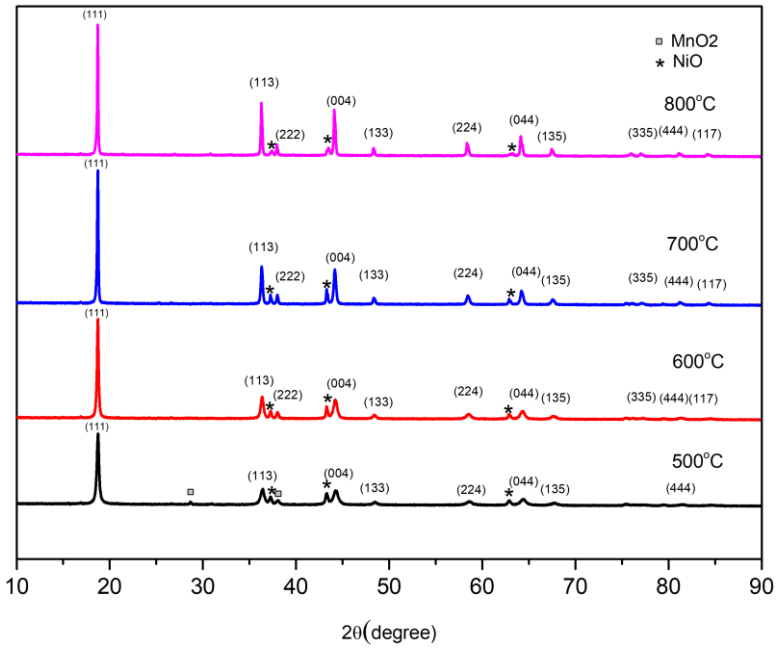


Figure 1. X-ray diffraction (XRD) pattern of LMNO synthesized at 500 °C, 600 °C, 700 °C, and 800 °C.

Copyright © 2026, Universitas Sebelas Maret, ISSN 1412-4092, e ISSN 2443-4183

Figure 1, XRD results show the various changes after sintering at 500 °C, 600 °C, 700 °C, and 800 °C. This is because the decomposing temperature of MnO2 is 535°C and this temperature is not reached during this heating process (Brostrøm *et al.*, 2020). With increasing sintering temperature, the changes in Miller index (111) phase become more obvious. But the NiO phase is not influenced even at the highest temperature of 800 °C, because the decomposition temperature of NiO is 1,950 °C. At 800 °C, the manganese phase is sufficiently reacted with the Lithium Manganese Oxide to give a unified phase. The XRD characterisation indicates that higher sintering temperatures are more conducive to the formation of Lithium Manganese Oxide, but the presence and nature of impurity phases can be different. Therefore, the variations in sintering temperature can have a strong effect on the crystal structure and the electrochemical performance of the LMNO samples. The increase in peak intensity with increasing sintering temperature indicates the increase in crystallinity. The P4332 structure of $LiMn_{1.5}Ni_{0.5}O_4$ is obtained when the sintering temperature is below 650 °C. The Ni^{2+} and Mn^{4+} ions are located at the octahedral 4a and 12b sites of the spinel lattice, respectively, which is an ordered P4332 configuration (Tiurin *et al.*, 2020). The most crystalline of the samples is LMNO 800 °C, which can be identified as a spinel with a cubic Fd3m symmetry, where the lithium ions are located at the tetrahedral (8a) sites, the transition metals (Mn and Ni) are situated at the octahedral (16d) sites, and the oxygen atoms are located at the 32e sites (Singh *et al.*, 2019). Many researchers have shown that the disordered Fd3m of $LiNi_{0.5}Mn_{1.5}O_4$ spinel has a much higher rate capability as compared to the ordered P4332 spinel due to its improved electronic and ionic conductivities (Walter *et al.*, 2020).

The morphological testing of LMNO samples obtained by solid-state method at temperatures of 500 °C, 600 °C, 700 °C, and 800 °C was carried out by FE-SEM, as shown in Figure 2. The particles at 500 °C show a basic block shaped morphology with pyramidal features and granules attached on their surfaces. The granules start to merge with base particles at 600 °C. By 700 °C most granules have fused into the base particles and the surface becomes smoother but irregular. At 800 °C the granules have disappeared and have formed denser, finer and more regular particles. The rise in temperature speeds up the sintering process, which decreases the particle size through compaction and pore elimination during heating (Garhi *et al.*, 2020). Figure 2 shows that the increase of the sintering temperature causes significant change in morphological surface.

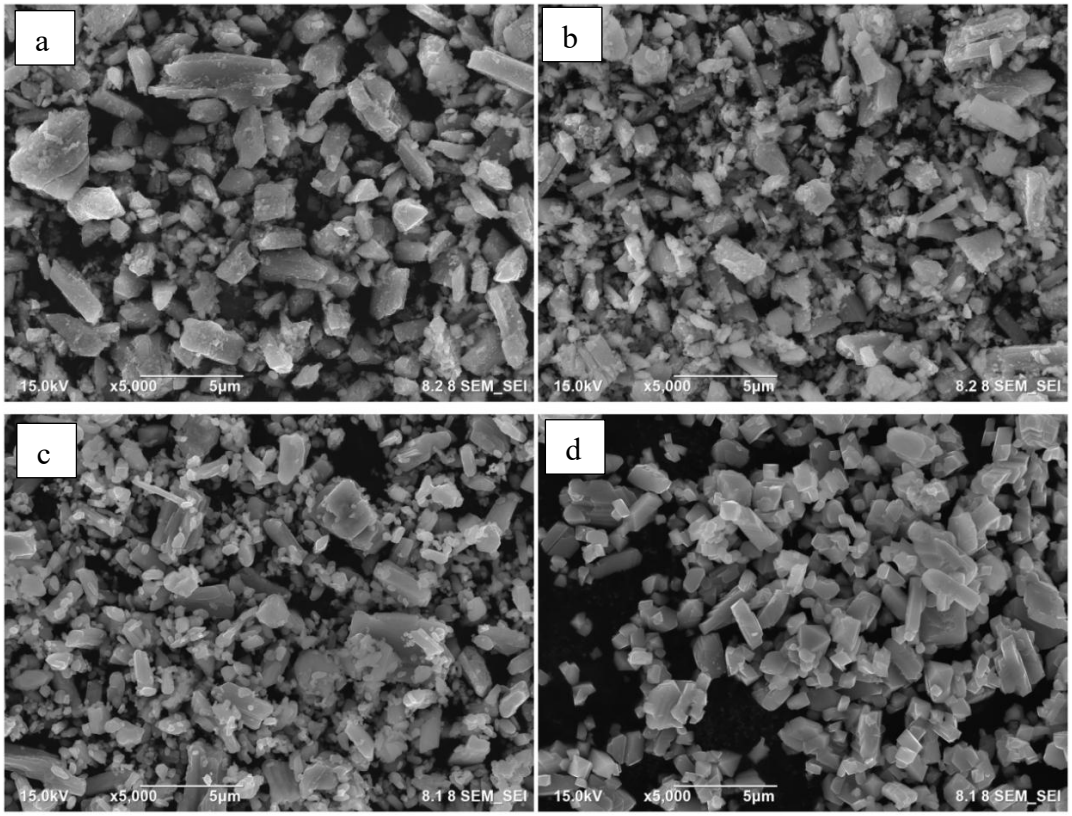


Figure 2. Results of FE-SEM characterization of LMNO synthesized at (a) 500 °C, (b) 600 °C, (c) 700 °C, and (d) 800 °C.

Copyright © 2026, Universitas Sebelas Maret, ISSN 1412-4092, e ISSN 2443-4183

The surface morphology appears smoothest at 800 °C due to the formation of LMO (Lithium Manganese Oxide) as confirmed by XRD. The results show that high temperatures induce the formation of LMO and enhance the intensity of its phase. Figure 3 shows that the average size of the surface morphology indicates that increasing the sintering temperature reduces the particle size, as the particle size of the calcined powders is directly proportional to the sintering temperature and time.

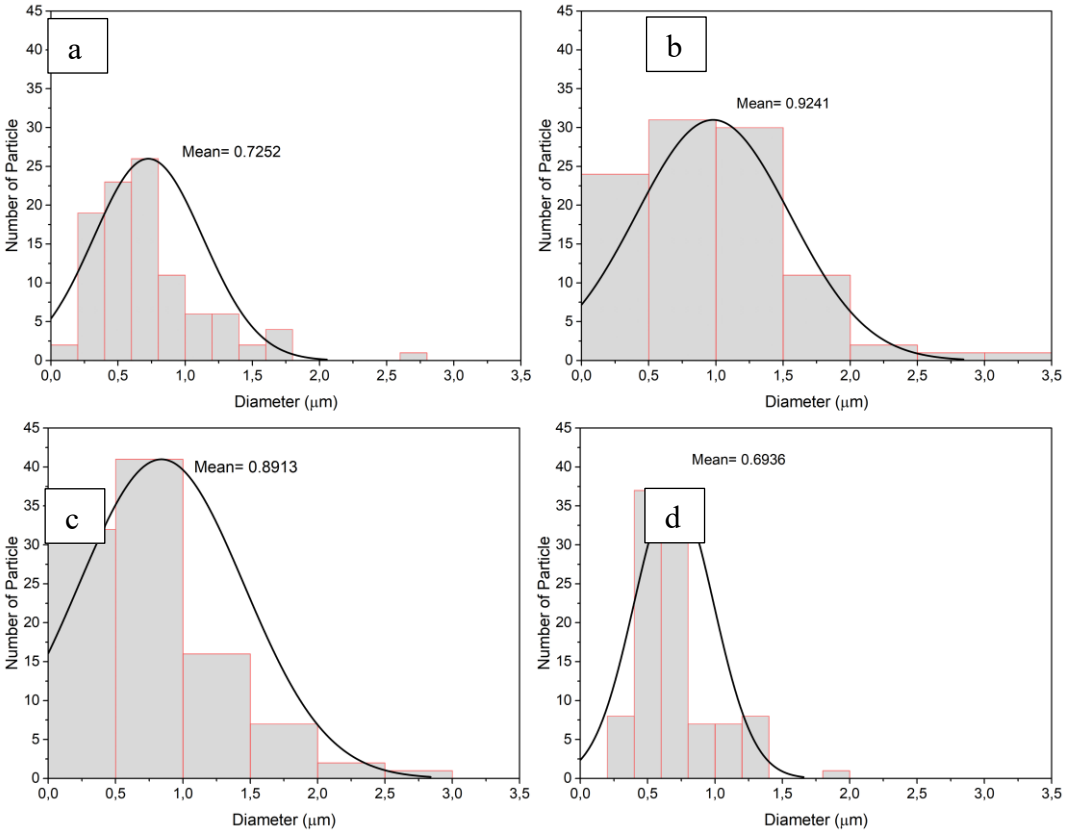


Figure 3. Average distribution of FE-SEM morphological sizes of LMNO synthesized at (a) 500 °C, (b) 600 °C, (c) 700 °C, and (d) 800 °C.

Energy-dispersive x-ray spectroscopy (EDS) analysis of LMNO synthesised by solid-state reaction at 500 – 800 °C confirmed Mn, Ni, and O as major component elements with no detectable extraneous impurities. The atomic percentage data in Table 1 show that Mn is relatively stable at 29.6 – 31.1 At%, while Ni gradually increases from 4.6 at% (500 °C) to 8.3 at% (800 °C) and the oxygen content slightly decreases from 65.2 at% to 61.4 At%. This trend indicates that higher calcination temperature favours Ni incorporation in the LMNO lattice and favours elemental diffusion. However, the Ni content at lower temperatures (500 – 700 °C) is still lower than the ideal stoichiometric value expected for $LiNi_{0.5}Mn_{1.5}O_4$, indicating incomplete reaction or possible phase segregation. The weight percentage results show a clear trend: Ni increases from 9.0 wt% to 15.5 wt% with increasing temperature, Mn decreases slightly and the oxygen content decreases accordingly. The elemental mapping images in Figure 4 also show a relatively uniform spatial distribution of Mn, NiX-ray, and O, especially at higher temperatures, which indicates improved compositional homogeneity and crystallisation. In general, the higher the synthesis temperature, the better the distribution of the elements and the approach to the targeted LMNO phase composition, though small deviations from the theoretical stoichiometry are still observed.

Table 1. EDS elemental composition (at% and wt%) of LMNO samples synthesized at 500 – 800 °C.

Sample	at%			wt%		
	Mn	Ni	O	Mn	Ni	O
LMNO 500	30.2	4.6	65.2	55.9	9	35.1
LMNO 600	**31.1**	**5.1**	**63.8**	**56.5**	**9.8**	**33.7**
LMNO 700	29.6	5.2	65.3	54.6	10.2	35.1
LMNO 800	**30.4**	**8.3**	**61.4**	**53.2**	**15.5**	**31.3**

Copyright © 2026, Universitas Sebelas Maret, ISSN 1412-4092, e ISSN 2443-4183

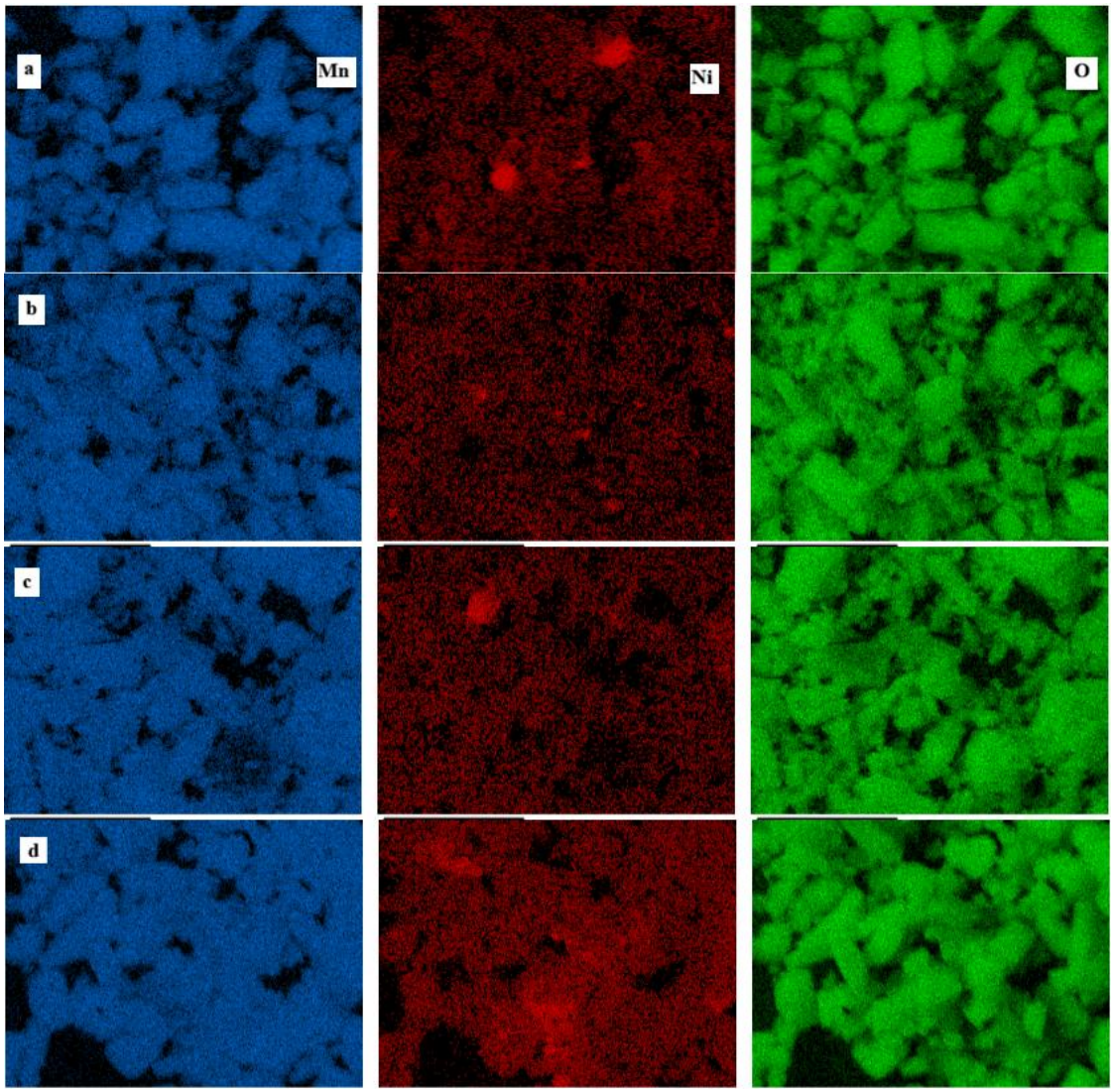


Figure 4. EDS elemental mapping of LMNO samples synthesized at 500 – 800 °C, showing the distribution of Mn, Ni, and O.

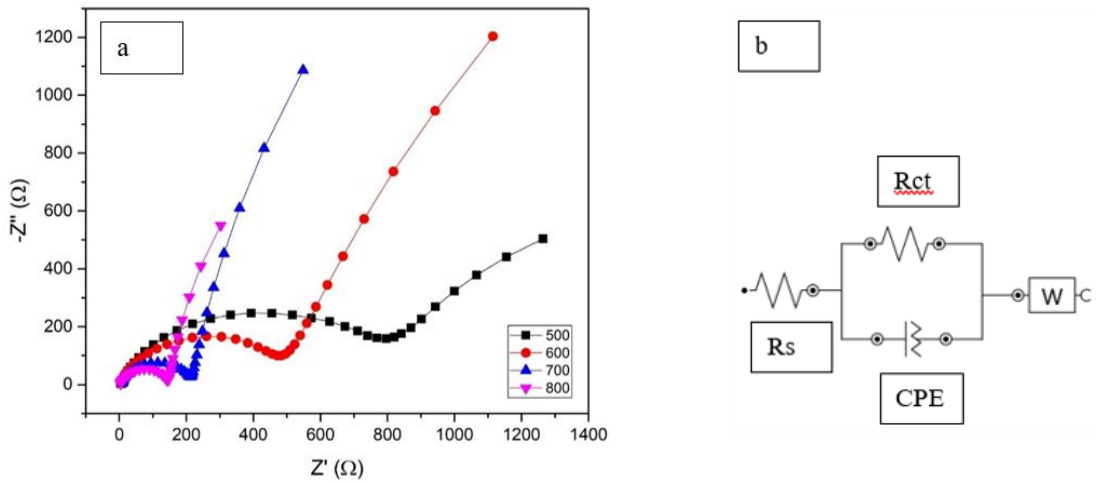


Figure 5. (a) Electrochemical test results of LMNO synthesized at 500 °C, 600 °C, 700 °C, and 800 °C and (b) Equivalent circuit for the samples.

The Electrochemical Impedance Spectroscopy (EIS) was performed to check the performance at fresh conditions after assembling the coin cell battery in Figure 5a. The EIS test is conducted based on impedance

Copyright © 2026, Universitas Sebelas Maret, ISSN 1412-4092, e ISSN 2443-4183

changes and semi-circle patterns at four sintering temperatures, 500 °C, 600 °C, 700 °C, and 800 °C. The resistance to ion transfer is shown as a semicircle in the graph and the ion intercalation (insertion) process is shown as a line at a 45° angle (Wei *et al.*, 2021).

The intercept on the Zre axis is equivalent to the resistance of the electrolyte (Re) and the electrode (Singh *et al.*, 2019). The semicircular high frequency value corresponds to the surface film resistance or the surface resistance value. The value of intermediate frequency is the charge transfer resistance (R_{CT}) and the low-frequency Warburg impedance (Zw) is related to the diffusion of Li^+ ions within the particles of the material (Wei *et al.*, 2021). The equivalent circuit used is shown in Figure 5b to fit the tested spectra, and the results are listed in Table 2.

Table 2. Calculation of resistance transfer resistance value (R_{CT}) and solution resistance value (R_S).

Samples	R_{CT} (Ω)	R_S (Ω)	Δ (Ω)
LMNO 500	768.742	5.48143	763.161
LMNO 600	484.643	3.81943	480.823
LMNO 700	214.156	7.39465	206.761
LMNO 800	146.035	3.47799	142.557

Four sintering temperatures (500 °C, 600 °C, 700 °C, and 800 °C) were compared and the higher sintering temperatures reduce the semicircle resistance due to the increasing LMNO phase. As shown in Table 2, the EIS test results show that the minimum impedance value is 146.035 Ω for charge transfer resistance and 142.557 Ω for total impedance at 800 °C. The total impedance is 206.761 Ω with charge transfer resistance of 214.156 Ω at 700 °C. It can be seen that the charge transfer resistance is 484.643 Ω and the total impedance is 480.823 Ω at 600 °C. The XRD results show that the LMO composition is 90% at 800 °C and the phase peak change is the largest compared to 700 °C, 600 °C, and 500 °C. The higher sintering temperature results in the ordering crystal structure and decrease in the ohmic resistance (Bojang and Wu, 2020; Walter *et al.*, 2020).

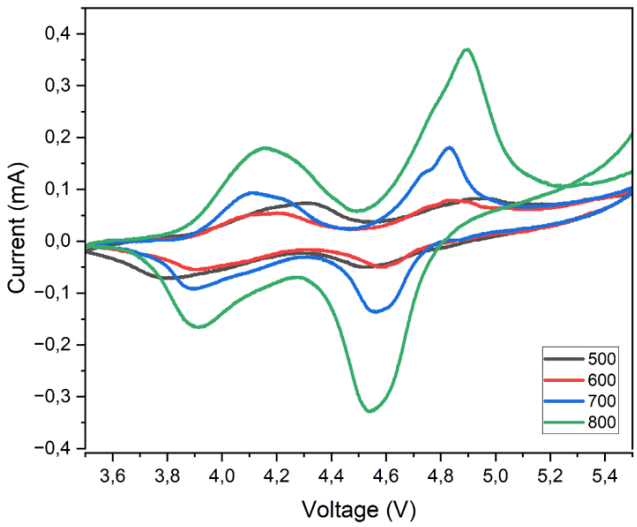


Figure 6. Cyclic Voltammetry test results of LMNO synthesized at 500 °C, 600 °C, 700 °C, and 800 °C.

Figure 6 shows the Cyclic Voltammetry electrochemical test used to observe voltage changes over time. Here, the CV test was carried out after the EIS test and before the CD test. From the results, it can be seen that the CV curve has two oxidation peaks and two reduction peaks. Two redox peaks are still observed, indicating that the sample still contains two phases. The raw material of NiO is a ceramic compound with high decomposition temperature (Garhi *et al.*, 2020). The first peak reveals redox peaks of Mn^{3+}/Mn^{4+} at about 3.9 V and 4.2 V (Saneifar *et al.*, 2020). The CV test at 800 °C was more stable and the peaks were higher due to the formation of LMNO at the second oxidation peak. Well defined and sharp redox peaks of Ni^{2+}/Ni^{3+} and Ni^{3+}/Ni^{4+} were observed with average anodic and cathodic peak potentials of ~ 4.875 V and ~ 4.56 V, respectively, for both electrodes. The redox peak for Mn is higher than Ni in samples 500 and 600 indicating that the LMNO phase has not been formed yet. The redox peak for Ni is higher in samples 700 and 800 indicating that LMNO has been formed.

Copyright © 2026, Universitas Sebelas Maret, ISSN 1412-4092, e ISSN 2443-4183

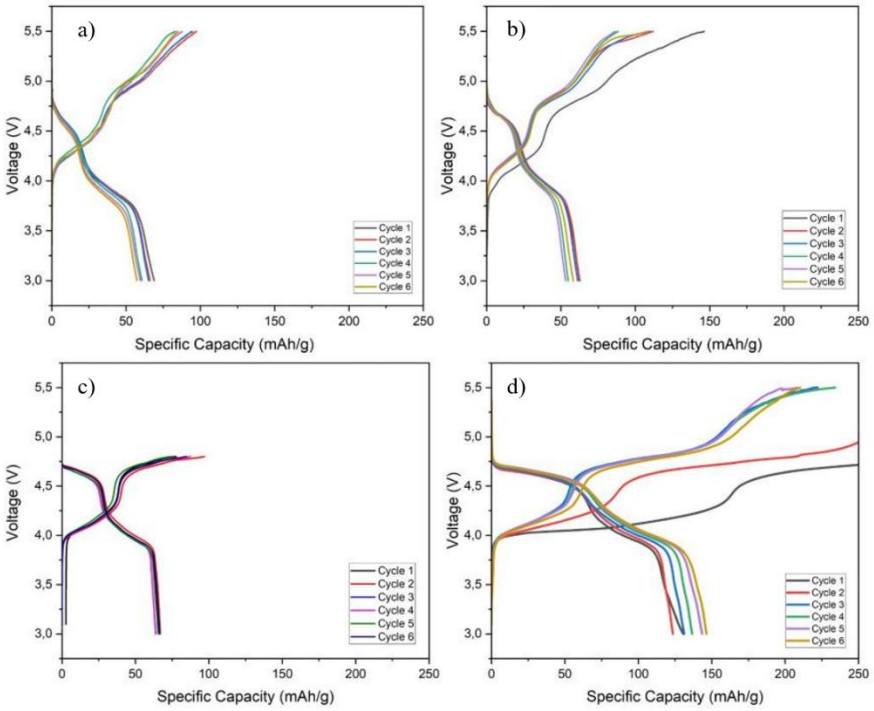


Figure 7. Charge-discharge test results of LMNO synthesized at (a) 500 °C, (b) 600 °C, (c) 700 °C and (d) 800 °C.

The unmodified LMNO cathode was tested for long-term stability by galvanostatic cycling between 3 and 5.5 V. Figure 7 displays the charge/discharge cycles of the electrode material at different sintering temperatures. It can be seen from Figure 7 that the sample has two different plateaus at ~4.0 V and ~4.5 V, which are corresponding to Mn^{4+}/Mn^{3+} and Ni^{2+}/Ni^{3+} transitions, respectively (Lv *et al.*, 2020). The charge/discharge data demonstrated that the lowest capacity values were for the samples heated at 500 °C and 600 °C with specific capacities of 68.81 $mAhg^{-1}$ and 62.40 $mAhg^{-1}$, respectively. The low capacities are ascribed to the lack of formation of LMNO and the minor impact of Ni on the capacity. Further capacity reduction to 50.78 $mAhg^{-1}$ was also observed at 700 °C in the sample and can also be attributed to the irregular morphology of the particles. Sample 800 °C however, showed a significant increase in capacity up to 146.44 $mAhg^{-1}$. The increase is attributed to the higher sintering temperature, leading to a greater formation of LMO and higher Ni content at 800 °C compared to the other temperatures. The 800 °C sample has a higher capacity value of 146.44 $mAhg^{-1}$ close to the theoretical capacity of LMNO of 148 $mAhg^{-1}$ which suggests good performance of the active electrolyte material. The charge-discharge tests reveal that the capacity values fall from the beginning of the cycle because of dissolution of transition metals in the electrolyte and high operating voltages, which can lead to electrolyte decomposition (Bhatia *et al.*, 2021).

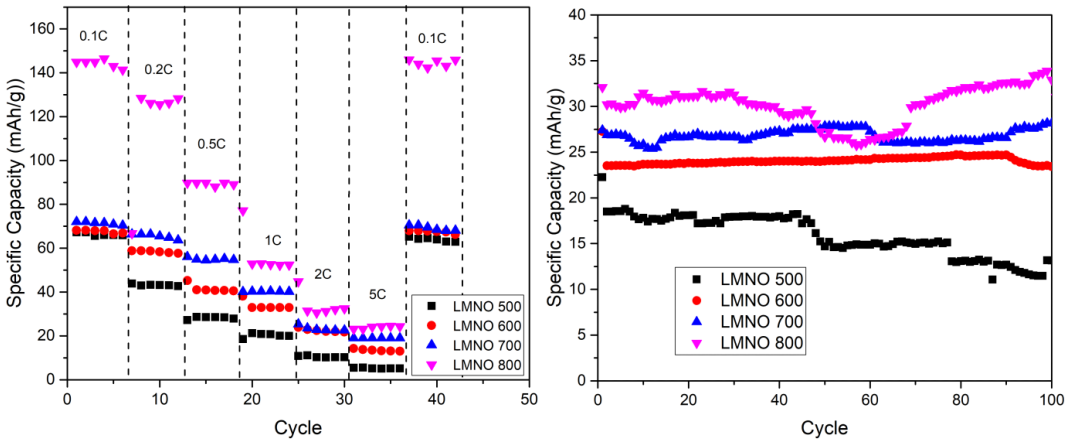


Figure 8. (a) Rate capability (0.1C – 5C) and (b) cycling performance of LMNO samples synthesized at 500, 600, 700, and 800 °C, showing specific capacity as a function of cycle number.

Copyright © 2026, Universitas Sebelas Maret, ISSN 1412-4092, e ISSN 2443-4183

Figure 8 depicts the rate capability and cycling performance of the spinel LMNO cathodes synthesised at 500 – 800 °C are noticeably enhanced as the calcination temperature increases. The LMNO 800 sample delivers the highest specific capacities at all C-rates and the best capacity retention upon return to low rates, followed by the samples synthesised at 700 and 600 °C, while LMNO 500 delivers the worst performance. This tendency is in agreement with previous reports that high calcination temperature improves crystallinity, cation ordering and electrochemical kinetics which enhance Li-ion diffusion and charge transfer, resulting in better rate capability and cycling stability of solid-state-synthesized $LiNi_{0.5}Mn_{1.5}O_4$ materials. For example, optimised high-temperature-synthesized spinel LNMO exhibits improved crystallinity and superb high-rate performance at 5 C even after long cycles, which underscores the vital effects of synthesis conditions on electrochemical properties. Recent work with high voltage spinel LNMO has also shown that engineering of particle structure and surface properties can greatly improve cycling retention over hundreds of cycles, highlighting the necessity of structural stability to obtain high rate and long term performance (Sun et al., 2009).

CONCLUSION

$LiMn_{1.5}Ni_{0.5}O_4$ has been successfully synthesised by a solid state reaction with different sintering temperature. XRD results showed that the highest Lithium Manganese Oxide composition (90.1%) was obtained for LMNO samples sintered at 800°C compared to samples sintered at other temperatures. The rise in composition is directly proportional to the rise in temperature. Further FE-SEM characterisation showed that higher sintering temperatures led to smoother surfaces and smaller particle sizes. The electrochemical analysis showed that LMNO sample sintered at 800 °C had better electrochemical performance with a resistance of 142.557 Ω and specific capacity of 146 $mAhg^{-1}$. This sample showed lower resistance, higher capacity and better retention of capacity as compared to samples sintered at lower temperatures. Thus, the increase in the sintering temperature improves the battery performance by reducing the resistance and optimising the capacity.

CONFLICT OF INTEREST

There is no conflict of interest in this article.

AUTHOR CONTRIBUTION

SP: Conceptualization, Methodology, Manuscript Review, and Manuscript Editing. VK: Research implementation guidance, and Manuscript Drafting. NJ: Laboratory Research, Processing Research Data: EIS, CV, and CD, and Manuscript Editing. AF: Laboratory Research, and Processing Research Data: XRD. EY: Manuscript Editing and Manuscript Review

ACKNOWLEDGEMENT

The authors expressed their gratitude for the financial support from the 2023 National Research and Innovation Agency (BRIN) House Program - Nanotechnology and Materials Research Organization.

DECLARATION OF GENERATIVE AI

During the process of writing this work, the authors used ChatGPT (OpenAI) for help with grammar correction, language improvement, and readability and clarity. The authors have full responsibility for the content of the published article after using this tool and have reviewed and amended it as necessary.

REFERENCES

Bhatia, A., Dridi Zrelli, Y., Pereira-Ramos, J.-P., and Baddour-Hadjean, R., 2021. Detailed Redox Mechanism and Self-Discharge Diagnostic of 4.9 V $LiMn_{1.5}Ni_{0.5}O_4$ Spinel Cathode Revealed by Raman Spectroscopy. *Journal of Materials Chemistry A*, 9, 13496–13505. https://doi.org/10.1039/D1TA00989C.

Bhatia, A., Pereira-Ramos, J.P., Emery, N., Laïk, B., Smith, R. I., and Baddour-Hadjean, R., 2020. An Exploratory Investigation of Spinel $LiMn_{1.5}Ni_{0.5}O_4$ as Cathode Material for Potassium-Ion Battery. *ChemElectroChem*, 7, 3385–3385. https://doi.org/10.1002/celc.202000889.

Bojang, A.A. and Wu, H.S., 2020. Characterization of Electrode Performance in Enzymatic Biofuel Cells Using Cyclic Voltammetry and Electrochemical Impedance Spectroscopy. *Catalysts*, 10, 782. https://doi.org/10.3390/catal10070782.

Copyright © 2026, Universitas Sebelas Maret, ISSN 1412-4092, e ISSN 2443-4183

Brostrøm, A., Kling, K. I., Hougaard, K. S., and Mølhave, K., 2020. Analysis of Electron Transparent Beam-Sensitive Samples Using Scanning Electron Microscopy Coupled with Energy-Dispersive X-Ray Spectroscopy. *Microscopy and Microanalysis*, 26, 373–386. https://doi.org/10.1017/S1431927620001464.

Gabrielli, G., Marinaro, M., Mancini, M., Axmann, P., and Wohlfahrt-Mehrens, M., 2017. A New Approach for Compensating the Irreversible Capacity Loss of High-Energy Si/C|$LiNi_{0.5}Mn_{1.5}O_4$ Lithium-Ion Batteries. *Journal of Power Sources*, 351, 35–44. https://doi.org/10.1016/j.jpowsour.2017.03.051.

Garhi, G., Aklalouch, M., Favotto, C., Mansori, M., and Saadoune, I., 2020. Coprecipitation Synthesis of Co-Doped $Limn_{1.5}ni_{0.5}o_4$ Material as 5 V Cathode of Li-Ion Batteries with Huge Rate Capability for High Power Applications. *Journal of Electroanalytical Chemistry*, 873, 114413. https://doi.org/10.1016/j.jelechem.2020.114413.

Lv, H., Huang, X., and Liu, Y., 2020. Analysis on Pulse Charging–Discharging Strategies for Improving Capacity Retention Rates of Lithium-Ion Batteries. *Ionics*, 26, 1749-1770. https://doi.org/10.1007/s11581-019-03404-8.

Saneifar, H., Zaghib, K., and Bélanger, D., 2020. Crown Ether Functionalized Conductive Carbon for High-Voltage Spinel $Limn_{1.5}ni_{0.5}o_4$/Graphite Cell. *ACS Applied Energy Materials*, 3, 647–657. https://doi.org/10.1021/acsaem.9b01854.

Singh, B., Kumar, S., and Kumar, P., 2019. Broken Translational and Rotational Symmetries in $LiMn_{1.5}Ni_{0.5}O_4$ Spinel. *Journal of Physics: Condensed Matter*, 31, 395701. https://doi.org/10.1088/1361-648X/ab2bdb.

Sun, Q., Li, X.-H., Wang, Z.-X., and Ji, Y., 2009. Synthesis and Electrochemical Performance of 5v Spinel $LiNi_{0.5}Mn_{1.5}O_4$ Prepared by Solid-State Reaction. *Transactions of Nonferrous Metals Society of China*, 19, 176–181. https://doi.org/10.1016/S1003-6326(08)60248-4.

Tiurin, O., Solomatin, N., Auinat, M., and Ein-Eli, Y., 2020. Atomic Layer Deposition (Ald) of Lithium Fluoride (Lif) Protective Film on Li-Ion Battery $LiMn_{1.5}Ni_{0.5}O_4$ Cathode Powder Material. *Journal of Power Sources*, 448, 227373. https://doi.org/10.1016/j.jpowsour.2019.227373.

Walter, M., Kovalenko, M. V., and Kravchyk, K. V., 2020. Challenges and Benefits of Post-Lithium-Ion Batteries. *New Journal of Chemistry*, 44, 1677–1683. https://doi.org/10.1039/C9NJ05682C.

Wei, A., Mu, J., He, R., Bai, X., Li, X., Zhang, L., Wang, Y., Liu, Z., and Wang, S., 2021. Enhanced Electrochemical Performance of $LiNi_{0.5}Mn_{1.5}O_4$ Composite Cathodes for Lithium-Ion Batteries by Selective Doping of K^+/Cl^- and K^+/F^-. *Nanomaterials*, 11, 2323. https://doi.org/10.3390/nano11092323.

Wu, W., Wang, S., Wu, W., Chen, K., Hong, S., and Lai, Y., 2019. A Critical Review of Battery Thermal Performance and Liquid Based Battery Thermal Management. *Energy Conversion and Management*, 182, 262–281. https://doi.org/10.1016/j.enconman.2018.12.051.

Xie, J. and Lu, Y.-C., 2020. A Retrospective on Lithium-Ion Batteries. *Nature Communications*, 11, 2499. https://doi.org/10.1038/s41467-020-16259-9.

Copyright © 2026, Universitas Sebelas Maret, ISSN 1412-4092, e ISSN 2443-4183